

## Supporting Information

### **Cation-exchange construction of ZnSe/Sb<sub>2</sub>Se<sub>3</sub> hollow microspheres coated by nitrogen-doped carbon with enhanced sodium ion storage capability**

Yuyu Wang,<sup>a†</sup> Dongxu Cao,<sup>b†</sup> Kailiang Zhang,<sup>c</sup> Wenpei Kang,<sup>b\*</sup> Xiaotong Wang,<sup>a</sup> Ping Ma,<sup>a</sup> Yufen Wan,<sup>a</sup> Dongwei Cao<sup>a</sup> and Daofeng Sun<sup>ab\*</sup>

<sup>a</sup> College of Science, China University of Petroleum (East China), Qingdao, Shandong 266580, People's Republic of China.

<sup>b</sup> School of Materials Science and Engineering, China University of Petroleum (East China), Qingdao, Shandong 266580, People's Republic of China.

<sup>c</sup> Shandong Institute for Product Quality Inspection, No 81, Shanda North Road, Jinan, Shandong 250100, People's Republic of China.

\*Email: wpkang@upc.edu.cn; dfsun@upc.edu.cn

The supporting information contains Fig. S1-S7 and Table S1-S3.

† These authors contributed equally to this work.

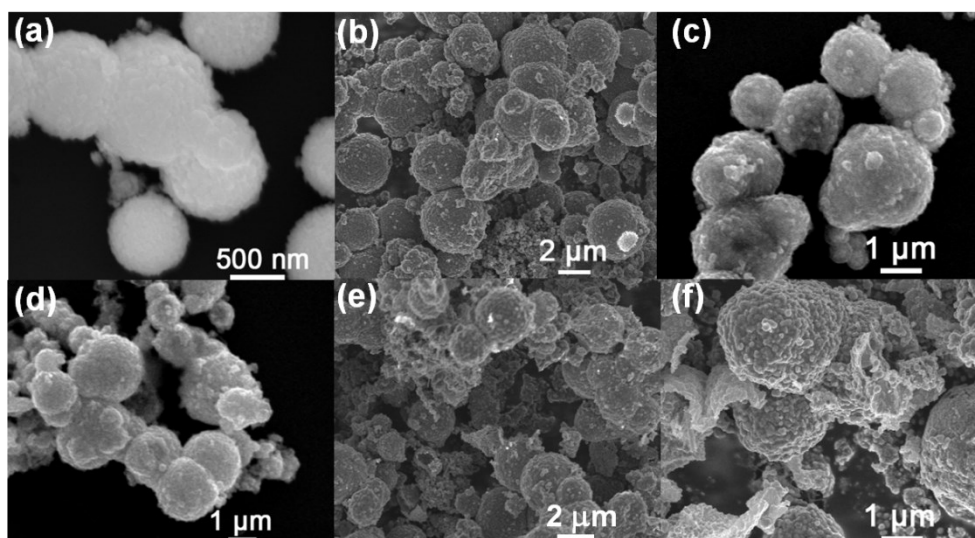


**Fig. S1** SEM images of (a) ZnSe precursor, (b) ZnSe@NC, (c) ZnSe/Sb<sub>2</sub>Se<sub>3</sub>@NC (10:1), (d) ZnSe/Sb<sub>2</sub>Se<sub>3</sub>@NC (50:1), (e) ZnSe/Sb<sub>2</sub>Se<sub>3</sub>@NC (100:1) and (f) ZnSe/Sb<sub>2</sub>Se<sub>3</sub>@NC (200:1).

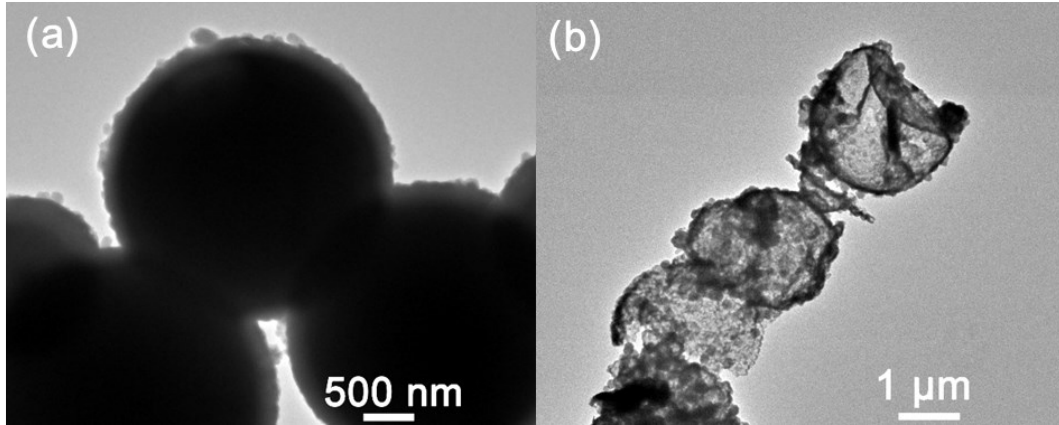


**Fig. S2** TEM images of (a) ZnSe@NC and (b) Sb<sub>2</sub>Se<sub>3</sub>@NC samples.

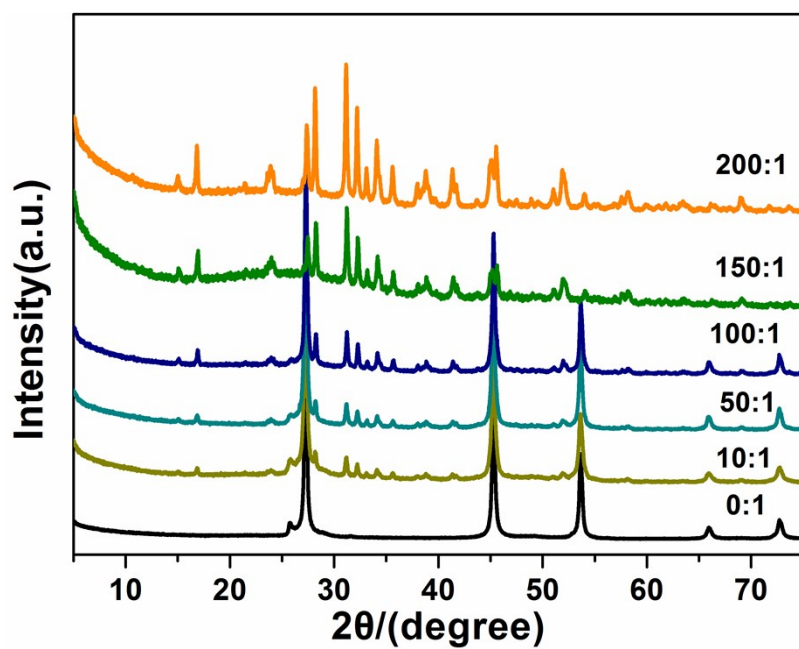


**Fig. S3** XRD curves for the sample obtained from different weight ratios of ZnSe@PDA : SbCl<sub>3</sub> during the ion exchange process.

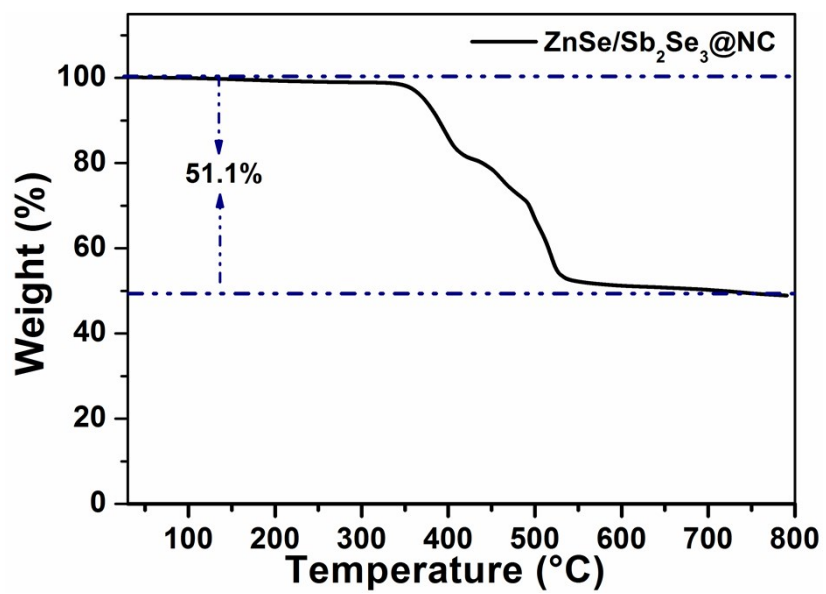
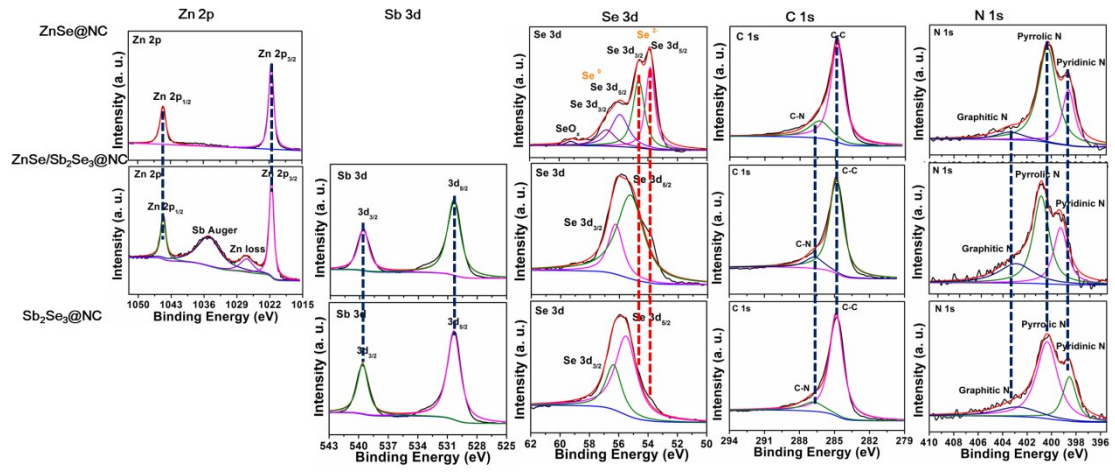
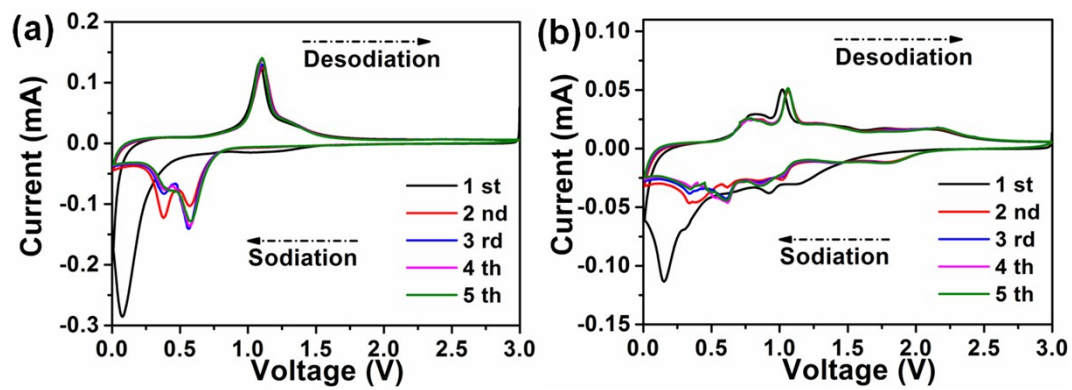


Fig. S4 TGA curve of the ZnSe/Sb<sub>2</sub>Se<sub>3</sub>@NC in the air atmosphere.



**Fig. S5.** Comparison of the XPS spectra for ZnSe@NC, Sb<sub>2</sub>Se<sub>3</sub>@NC and ZnSe/Sb<sub>2</sub>Se<sub>3</sub>@NC.



**Fig. S6** CV curves for (a) ZnSe@NC and (b) Sb<sub>2</sub>Se<sub>3</sub>@NC electrodes at the scan rates of 0.1 mV S<sup>-1</sup>.

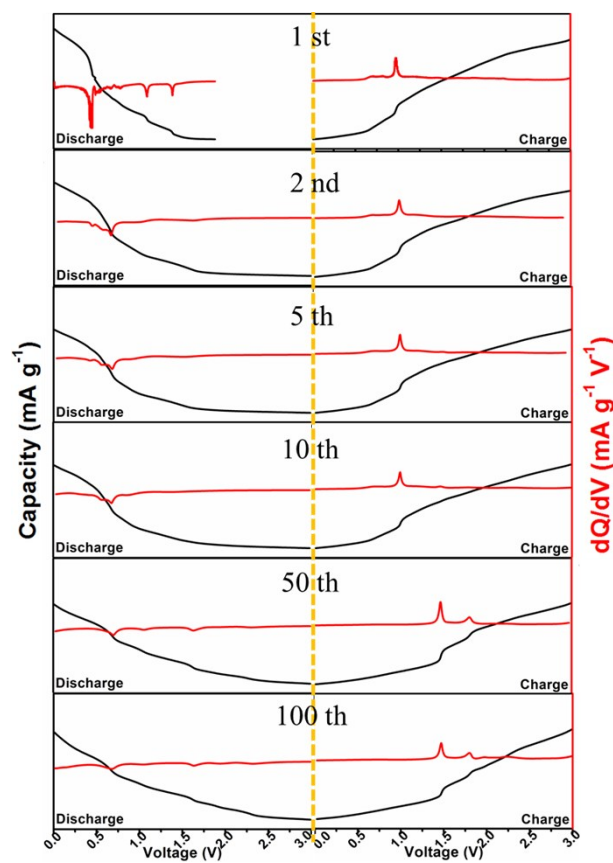


**Fig. S7** The selected discharge/charge profiles and the corresponding  $dQ/dV$  curves at  $0.5 \text{ A g}^{-1}$  ( $0.05 \text{ A g}^{-1}$  for the initial cycle) of  $\text{ZnSe/Sb}_2\text{Se}_3@\text{NC}$ .



**Table S1** ICP result of the ZnSe/Sb<sub>2</sub>Se<sub>3</sub>@NC hollow microsphere.

Analyte	Conc.Units
Zn	17.69 mg/L
Sb	13.36 mg/L

**Table S2** The at% and wt% of the N element in the samples.

		ZnSe@NC	ZnSe/Sb <sub>2</sub> Se <sub>3</sub> @NC	Sb <sub>2</sub> Se <sub>3</sub> @NC
N	at%	9.76	8.90	8.42
	wt%	8.71	5.57	5.61

**Table S3** Initial capacity loss comparisons with other selenide anodes and ZnSe/Sb<sub>2</sub>Se<sub>3</sub>@NC hollow microsphere as anode materials for SIBs.

Materials	Initial discharge capacity	Initial charge capacity	Initial Coulombic efficiency	References
ZnSe/Sb <sub>2</sub> Se <sub>3</sub> @NC hollow microsphere	570.5 mAh g <sup>-1</sup>	516.5 mAh g <sup>-1</sup>	90.5%	Our work
CoSe <sub>2</sub> /(NiCo)Se <sub>2</sub> box-in-box hollow nanocubes	661 mAh g <sup>-1</sup>	574 mAh g <sup>-1</sup>	79.6%	[1]
MoSe <sub>2</sub> /C nanotubes encapsulated with CoSe <sub>2</sub> nanoparticles	590 mAh g <sup>-1</sup>	450 mAh g <sup>-1</sup>	76.3%	[2]
SnSe/C wrapped Within N-doped graphene	652.6 mAh g <sup>-1</sup>	486.1 mAh g <sup>-1</sup>	74.49%	[3]
rGO-overcoated Sb <sub>2</sub> Se <sub>3</sub> nanorods	940 mAh g <sup>-1</sup>	682 mAh g <sup>-1</sup>	72.6%	[4]
CoSe <sub>2</sub> nanobuds encapsulated into boron and nitrogen codoped graphene (BCN) nanotubes	926 mAh g <sup>-1</sup>		68.5%	[5]
FeSe <sub>2</sub> @C hollow nanocubes	858 mAh g <sup>-1</sup>	539 mAh g <sup>-1</sup>	62.8%	[6]
ZnSe-NC@CoSe <sub>2</sub> -NC polyhedrons	882.6 mAh g <sup>-1</sup>	502.5 mAh g <sup>-1</sup>	56.9%	[7]
N-ZnSe@rGO polyhedra	1022 mAh g <sup>-1</sup>	562 mAh g <sup>-1</sup>	54.9%	[8]

## Notes and references

- 1 S. K. Park, J. K. Kim and Y. C. Kang, Metal-organic framework-derived  $\text{CoSe}_2/(\text{NiCo})\text{Se}_2$  box-in-box hollow nanocubes with enhanced electrochemical properties for sodium-ion storage and hydrogen evolution, *J. Mater. Chem. A*, 2017, **5**, 18823-18830.
- 2 J. Gao, Y. Li, L. Shi, J. Li and G. Zhang, Rational design of hierarchical nanotubes through encapsulating  $\text{CoSe}_2$  nanoparticles into  $\text{MoSe}_2/\text{C}$  composite shells with enhanced lithium and sodium storage performance, *ACS Appl. Mater. Interfaces*, 2018, **10**, 20635-20642.
- 3 C. Lu, Z. Li, Z. Xia, H. Ci, J. Cai, Y. Song, L. Yu, W. Yin, S. Dou, J. Sun and Z. Liu, Confining MOF-derived  $\text{SnSe}$  nanoplatelets in nitrogen-doped graphene cages via direct CVD for durable sodium ion storage, *Nano Res.*, 2019, **12**, 3051-3058.
- 4 X. Ou, C. Yang, X. Xiong, F. Zheng, Q. Pan, C. Jin, M. Liu and K. Huang, A new rGO-overcoated  $\text{Sb}_2\text{Se}_3$  nanorods anode for  $\text{Na}^+$  battery: in situ X-Ray diffraction study on a live sodiation/desodiation process, *Adv. Funct. Mater.*, 2017, **27**, 1606242.
- 5 H. Tabassum, C. Zhi, T. Hussain, T. Qiu, W. Aftab and R. Zou, Encapsulating trogtalite  $\text{CoSe}_2$  nanobuds into BCN nanotubes as high storage capacity sodium ion battery anodes, *Adv. Energy Mater.*, 2019, **9**, 1901778.
- 6 H. Fan, H. Yu, Y. Zhang, J. Guo, Z. Wang, H. Wang, N. Zhao, Y. Zheng, C. Du, Z. Dai, Q. Yan and J. Xu, 1D to 3D hierarchical iron selenide hollow nanocubes assembled from  $\text{FeSe}_2@\text{C}$  core-shell nanorods for advanced sodium ion batteries, *Energy Storage Mater.*, 2018, **10**, 48-55.
- 7 X. Hu, X. Liu, K. Chen, G. Wang and H. Wang, Core-shell MOF-derived N-doped yolk-shell carbon nanocages homogenously filled with  $\text{ZnSe}$  and  $\text{CoSe}_2$  nanodots as excellent anode materials for lithium- and sodium-ion batteries, *J. Mater. Chem. A*, 2019, **7**, 11016-11037.
- 8 X. Liu, Y. Liu, M. Feng and L.-Z. Fan, MOF-derived and nitrogen-doped  $\text{ZnSe}$  polyhedra encapsulated by reduced graphene oxide as the anode for lithium and sodium storage, *J. Mater. Chem. A*, 2018, **6**, 23621-23627.